RadioGraphics

Pediatric FDG PET/CT: Physiologic Uptake, Normal Variants, and Benign Conditions[1]

Amer Shammas, MD • Ruth Lim, MD[2] • Martin Charron, MD

CME FEATURE

See the questionnaire on pp 1537–1544.

LEARNING OBJECTIVES FOR TEST 5

After reading this article and taking the test, the reader will be able to:

- Describe the normal distribution of ^{18}F FDG uptake in children.
- Recognize normal variants at pediatric ^{18}F FDG PET/CT.
- Discuss common ^{18}F FDG–avid benign lesions and causes of imaging artifacts.

TEACHING POINTS

See last page

Positron emission tomography (PET) with 2-[fluorine-18]fluoro-2-deoxy-D-glucose (FDG) is increasingly being used in the evaluation of pediatric oncology patients. However, the normal distribution of ^{18}F FDG uptake in children is unique and may differ from that in adults. A number of physiologic variants are commonly encountered, including normal physiologic uptake in the head and neck, heart, breast, thymus, liver, spleen, gastrointestinal tract, genital system, urinary collecting system, bone marrow, muscles, and brown adipose tissue. Benign lesions with increased ^{18}F FDG uptake are also frequently seen and can be misinterpreted as malignancies. In addition, the use of combined PET/computed tomographic (CT) scanners is associated with pitfalls and artifacts such as attenuation correction and misregistration. Proper interpretation of pediatric ^{18}F FDG PET/CT studies requires knowledge of the normal distribution of ^{18}F FDG uptake in children, as well as of the aforementioned physiologic variants, benign lesions, and PET/CT-related artifacts. Knowing these potential causes of misinterpretation can increase accuracy in PET image interpretation, decrease the number of unnecessary follow-up studies or procedures, and improve patient treatment.

Abbreviations: CSF = colony-stimulating factor, FDG = 2-[fluorine-18]fluoro-2-deoxy-D-glucose, MIP = maximum-intensity-projection, SUV = standardized uptake value

RadioGraphics 2009; 29:1467–1486 • **Published online** 10.1148/rg.295085247 • **Content Codes:** CT NM PD

[1]From the Department of Diagnostic Imaging, Hospital for Sick Children, University of Toronto, 555 University Ave, Toronto, ON, Canada M5G 1X8. Recipient of a Certificate of Merit award for an education exhibit at the 2007 RSNA Annual Meeting. Received December 22, 2008; revision requested February 25, 2009 and received March 30; accepted April 7. R.L. is a consultant with New England PET Imaging Systems; all other authors have no financial relationships to disclose. **Address correspondence to** A.S. (e-mail: *amershammas@yahoo.com*).

[2]**Current address:** Department of Radiology, Massachusetts General Hospital, Harvard Medical School, Boston, Mass.

Introduction

Positron emission tomography (PET) with 2-[fluorine-18]fluoro-2-deoxy-D-glucose (FDG) has been established as an effective modality for detecting various types of cancer and is rapidly becoming the standard modality of care for many cancers in adults (1–3). ^{18}F FDG PET is also being applied with increasing frequency in the evaluation of children with various malignancies (4–8). However, a number of pitfalls are commonly encountered with ^{18}F FDG PET in children, including uptake in benign lesions and normal physiologic activity, leading to possible misinterpretation as malignancy and inaccurate disease staging (9,10). A thorough knowledge and understanding of the normal distribution of ^{18}F FDG uptake in children, normal variants at pediatric ^{18}F FDG PET/computed tomography (CT), and PET/CT artifacts is essential for accurate image interpretation.

In this article, we discuss and illustrate the normal distribution of ^{18}F FDG uptake in children, a variety of physiologic variants in distribution, benign lesions that could be misinterpreted as malignancies, and the most common artifacts associated with PET/CT performed in pediatric oncology patients.

Imaging Techniques and Considerations

Use of ^{18}F FDG

^{18}F FDG is a glucose analog labeled with a positron-emitting isotope, F (fluorine)–18. It is transported into cells by glucose transporters, phosphorylated by hexokinase, and trapped within the cell. Malignant tissues accumulate ^{18}F FDG more avidly than do normal tissues due to their increased glucose metabolism rate, increased expression of glucose transporters, and highly active hexokinase bound to tumor mitochondria compared with normal tissue (11). ^{18}F FDG uptake is also known to occur in nonmalignant inflammation and infection (12,13). Increased uptake in inflammation is due to an increased number of glucose transporters. In addition, the affinity of glucose transporters for deoxyglucose is apparently increased by various cytokines and growth factors, a phenomenon that has not been observed in tumors (12). Imaging of inflammation with ^{18}F FDG PET is also based on the fact that infiltrated granulocytes and tissue macrophages use glucose as an energy source. When these granulocytes and macrophages are activated (ie, when inflammation occurs), metabolism—and, thus, FDG uptake—increases (14,15).

Indications

Although data are limited, an increasing number of reports are being published regarding the clinical utility and impact of ^{18}F FDG PET/CT in pediatric oncology (4). The most common indications for ^{18}F FDG PET in pediatric oncology include lymphoma, sarcoma, and neuroblastoma (16). ^{18}F FDG PET can be used in lymphoma (both Hodgkin and non-Hodgkin types) for staging, evaluation of response to therapy, restaging, assessment of residual masses after therapy, biopsy planning, and planning of radiation therapy (4,5,16). It is also used in osteosarcoma, Ewing sarcoma, and soft-tissue sarcomas for similar purposes. ^{18}F FDG PET is used in neuroblastoma, especially in MIBG (metaiodobenzylguanidine)–negative cases or cases of opsoclonus-myoclonus syndrome in which no primary tumor is detected at conventional imaging (9,16,17). Less common reasons for performing ^{18}F FDG PET in pediatric oncology patients include the evaluation of germ cell tumors, hepatoblastoma, Wilms tumor, malignancy from an unknown primary tumor, and neurofibromatosis type 1 for suspected malignant transformation of plexiform neurofibroma (16,18). In an early series at our institution, 52% of 54 ^{18}F FDG PET/CT studies were performed for lymphoma, 14% for neuroblastoma, 11% for sarcoma, and 7% for posttransplantation lymphoproliferative disorder.

Patient Preparation

Specific information is required for optimal interpretation of FDG PET/CT images, such as clinical history; results of previous imaging studies; history of surgery, chemotherapy, or radiation therapy; and presence of a central venous or drainage catheter (16). A thorough explanation of the procedure should be given to the patient and his or her parents. The child should fast for at least 4–6 hours before the study, but should drink water to maintain good hydration if anesthesia or sedation is not indicated (16,18). Intravenously performed hydration during the uptake period may be achieved with 0.9% saline solution (18). In infants, radiotracer injection should be timed as close as possible to breast or bottle feeding; a feed may be given from 30 minutes after injection (16,18). The fasting blood glucose level needs to be determined prior to ^{18}F FDG injection, with the preferred level being lower than 7 mmol/L. If the blood glucose level is higher than 7 mmol/L, the supervising physician should be notified so that a decision can be made whether to proceed with the radiotracer injection (18). Local anesthetic cream can be used to reduce the discomfort caused by the intravenous catheter (16). Children with known or suspected tumors are usually imaged approximately 1–2 hours after the intravenous administration of ^{18}F FDG (18). The optimal ^{18}F FDG distribution phase is controversial. Many facilities begin acquiring images 60–90 minutes after ^{18}F FDG administration. Some facilities obtain a second set of images to assess the change in uptake over time. The duration of the ^{18}F FDG uptake period should be kept constant whenever possible (19). A dose of 5.18–7.4 MBq/kg (0.14–0.20 mCi/kg) has been recommended for pediatric oncology patients (19). After injection, children should avoid exercising, talking, or chewing. They should be kept warm during the uptake phase with an adequately heated room and the use of warm blankets and clothing. This approach may help reduce radiotracer uptake in thermogenic brown fat. At our institution, children spend the uptake period watching a movie on DVD (digital video disk) while seated in a reclining armchair in a warm, quiet, dimly lit room.

The need for a sedative or anesthetic must be assessed on a case-by-case basis in children who cannot remain motionless in the scanner for at least 15–20 minutes. Patient motion will interrupt the PET study, resulting in inadequate image quality (16). Generally, sedation or anesthesia protocols are variable and are performed in accordance with institutional guidelines. Guidelines from the American College of Radiology and the American Academy of Pediatrics can help in developing an institutional sedation protocol (20).

Bladder catheterization may be used to reduce accumulated urinary radiotracer activity in the bladder (19). However, catheters are neither routinely used nor generally recommended in pediatric patients because catheterization increases the risk of infection and causes additional stress for children (16). Loop diuretics such as furosemide (0.5–1 mg/kg; maximum dose, 20 mg) can be given to enhance diuresis and reduce activity in the urinary tract. However, furosemide might be more valuable with dedicated PET-only scanners (16,19). Combined PET/CT provides additional anatomic information that is often sufficient to accurately localize the focal area of increased radiotracer uptake in the urinary tract (16).

Combined PET/CT

A field of view extending from the skull base to the midthighs is usually sufficient. However, in neuroblastoma, sarcoma, or lymphoma with suspected skeletal or bone marrow involvement, the upper and lower extremities as well as the skull should be included (16). With combined PET/CT scanners, attenuation coefficients obtained from the CT component are used to generate attenuation-corrected PET scans. The additional radiation exposure to the pediatric patient from the CT component of the examination has become an issue of concern (16). Children should be evaluated individually to determine if CT is to be used for attenuation correction and anatomic localization only (very low-dose CT), or if diagnostic quality is needed (routine-dose CT). The CT tube current may be reduced to 25–35

mAs (pitch, 1.5) in most children in whom CT is used for attenuation correction and localization only (18). According to the literature on adult patients, the whole-body effective dose for low-dose CT performed at 30–32.5 mAs is 10%–20% of that for routine-dose CT (1.3–2.4 mSv versus 14.1–17.6 mSv) (21). Recent pediatric research indicates that adequate attenuation correction can be achieved with ultra-low-dose CT (80 kVp, 5 mAs, 1.5:1 pitch), representing a 100-fold dose reduction relative to routine-dose diagnostic CT (22). However, the minimum CT dose needed to provide adequate anatomic correlation with the PET findings was not evaluated in this research.

At our institution, children with known or suspected tumors are imaged approximately 1 hour after the intravenous administration of ^{18}F FDG (5.18 MBq/kg [0.14 mCi/kg]; maximum, 370 MBq [10 mCi]). Blood glucose level is checked prior to injection of the radiotracer. Patients rest in a quiet room while covered in warm blankets during the uptake period. No premedication is used to minimize brown adipose tissue or muscle uptake. When required, either conscious sedation or general anesthesia is induced per standard department protocol. When clinically indicated, diagnostic-quality intravenous contrast material–enhanced CT is performed and the resultant CT scans are used for attenuation correction (23–25). Otherwise, only very low-dose nonenhanced CT scans are acquired for attenuation correction and anatomic localization. No oral contrast material is used. PET/CT images are obtained on a 16-section germanium oxyorthosilicate scanner (GEMINI GXL; Philips, Cleveland, Ohio). CT is performed prior to the acquisition of PET data in a single step with the patient supine and, if possible, with the patient's arms positioned above the head. Caudocranial three-dimensional PET data are subsequently acquired (1½ minutes per bed position).

Normal Distribution of ^{18}F FDG Uptake

The normal physiologic accumulation of ^{18}F FDG in the body is based on glucose metabolism, which can be variable. Physiologic uptake is normally seen in the brain, heart, liver, spleen, gastrointestinal tract, urinary collecting system (including the bladder), and bone marrow (Fig 1).

Figure 1. Coronal ^{18}F FDG PET scan shows normal physiologic ^{18}F FDG uptake in the brain, heart, liver, spleen, urinary collecting system (including the bladder), and bone marrow. Note the markedly intense activity in the brain compared with the activity in the rest of the body.

Normal Distribution and Physiologic Variants of ^{18}F FDG Uptake in Children

The normal distribution and physiologic variants of ^{18}F FDG uptake in children differ from those in adults, and it is important that they be recognized so as to avoid misinterpretation (9,20).

Head and Neck

The most intense ^{18}F FDG activity is present in the normal cerebral cortex and basal ganglia because the brain is dependent on glycolytic metabolism as a source of energy (Fig 1). Brain metabolism may account for as much as 20% of whole-

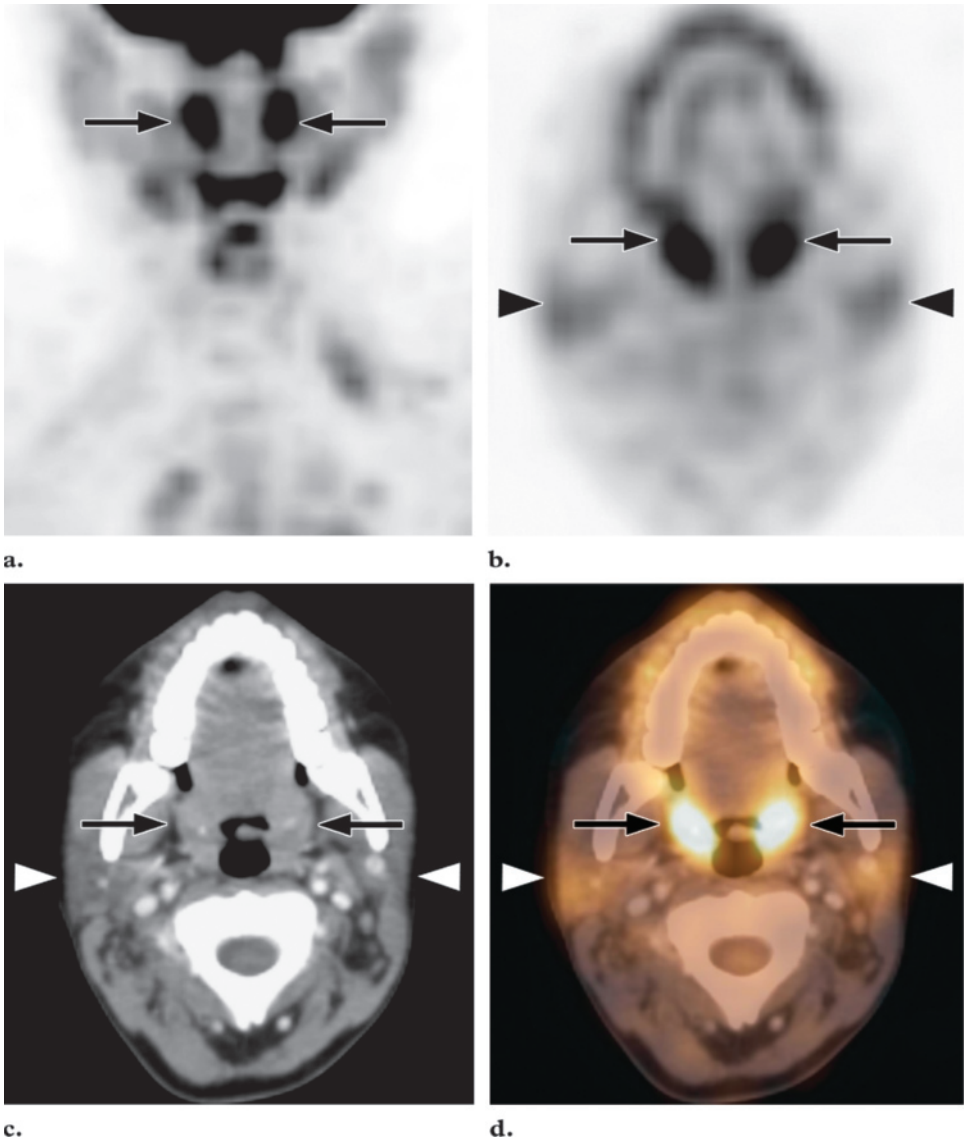

Figure 2. Maximum-intensity-projection (MIP) FDG PET image **(a)** and transverse FDG PET **(b)**, CT **(c)**, and fused PET/CT **(d)** images show marked and symmetric uptake in normal tonsils (arrows) as well as bilateral mild uptake in the parotid glands (arrowheads in **b–d**).

body metabolism in the fasting state (10). The total uptake in the brain represents approximately 6% of the injected dose of ^{18}F FDG (26).

Mild to moderate uptake is usually seen in the adenoids, in the tonsils, and at the base of the tongue due to the physiologic activity of lymphatic tissue in the Waldeyer ring (10). However, markedly intense uptake can be seen in the Waldeyer ring (Fig 2) (27)—especially in children, due to high physiologic activity of these lymphatic tissues that peaks at 6–8 years of age, after which time it diminishes. These areas of normal ^{18}F FDG activity in children should not necessarily be interpreted as disease. Usually, the symmetric pattern of physiologic tonsillar and adenoidal uptake is helpful in identifying this normal variant (28). The soft palate can also show intense radiotracer uptake (29).

Uptake in the salivary glands is variable but typically mild to moderate (Fig 3) (10). Nakamoto et al (29) reported mild to moderate parotid gland uptake in 51% of patients and intense parotid

Teaching Point

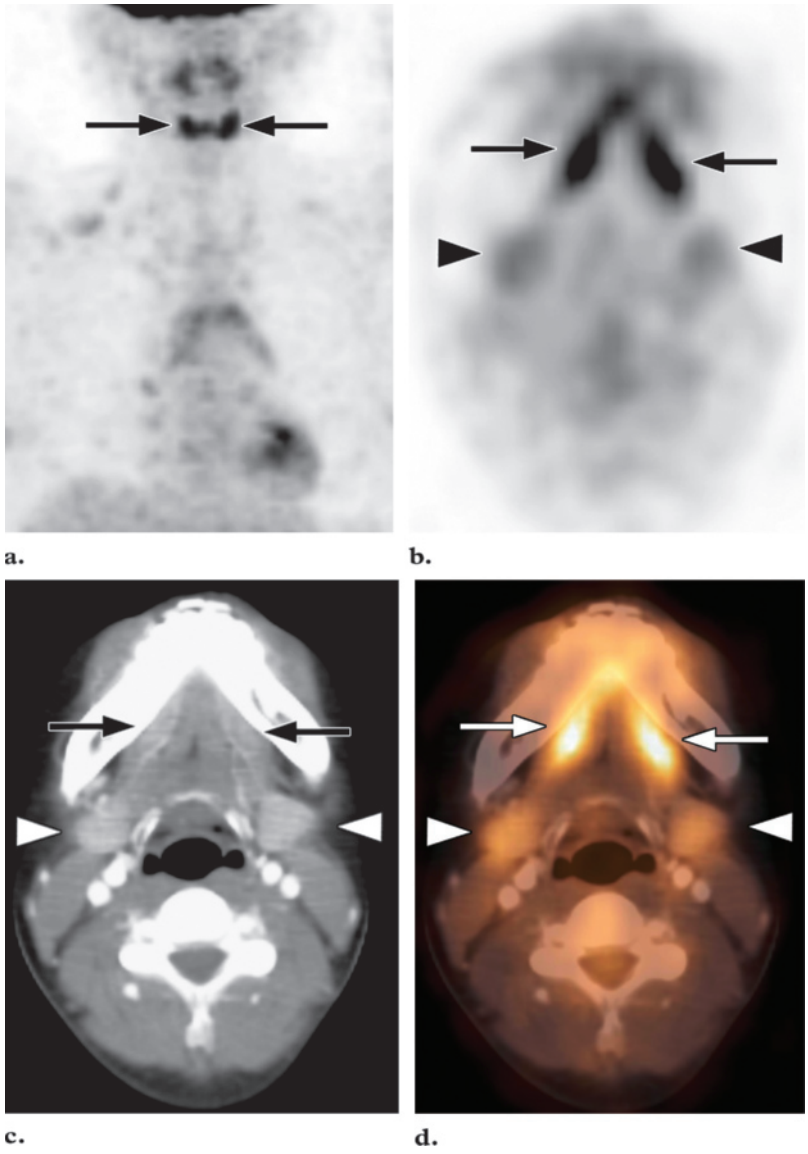

Figure 3. MIP FDG PET image **(a)** and transverse FDG PET **(b)**, CT **(c)**, and fused PET/CT **(d)** images show markedly increased uptake in the sublingual glands (arrows) and mildly increased uptake in the submandibular glands (arrowheads in **b–d**).

gland uptake in 14%. The uptake in the submandibular and sublingual glands was variable, with positive rates of 53% and 72%, respectively (29). Diffusely increased salivary gland uptake can also be seen after chemotherapy or radiation therapy (27). ^{18}F FDG uptake in the salivary glands can be asymmetric due to acute inflammation following recent surgery or radiation therapy. However, radiation therapy may eventually cause decreased uptake on the affected side (10).

The larynx and vocal cords usually show either no uptake or mild symmetric uptake, which may have an inverted U shape (Fig 4) (27,29). It is important to instruct children not to talk during the uptake phase, since excessive talking may cause prominent activity in the laryngeal structures (27). Asymmetric vocal cord uptake suggests the possibility of disease such as malignancy, posttherapy change, or unilateral vocal cord paralysis (27).

Variable ^{18}F FDG uptake that corresponds to the genioglossus muscle in the floor of the mouth, which keeps the tongue forward when the patient is supine, can sometimes be noted. Placing the patient upright during the uptake phase can minimize this uptake (30). Muscle activity can also be identified at the convergence of the extraocular muscles, as well as along the length of these muscles (Fig 5) (27).

Occasionally, incidental diffuse symmetric uptake can be seen in clinically euthyroid patients (10,27). In our experience, this is a relatively rare occurrence in children. However, such diffuse thyroid uptake may represent Graves disease or thyroiditis. Focal thyroid uptake can be seen in benign thyroid nodules or malignancies, and further work-up is warranted in such cases (27).

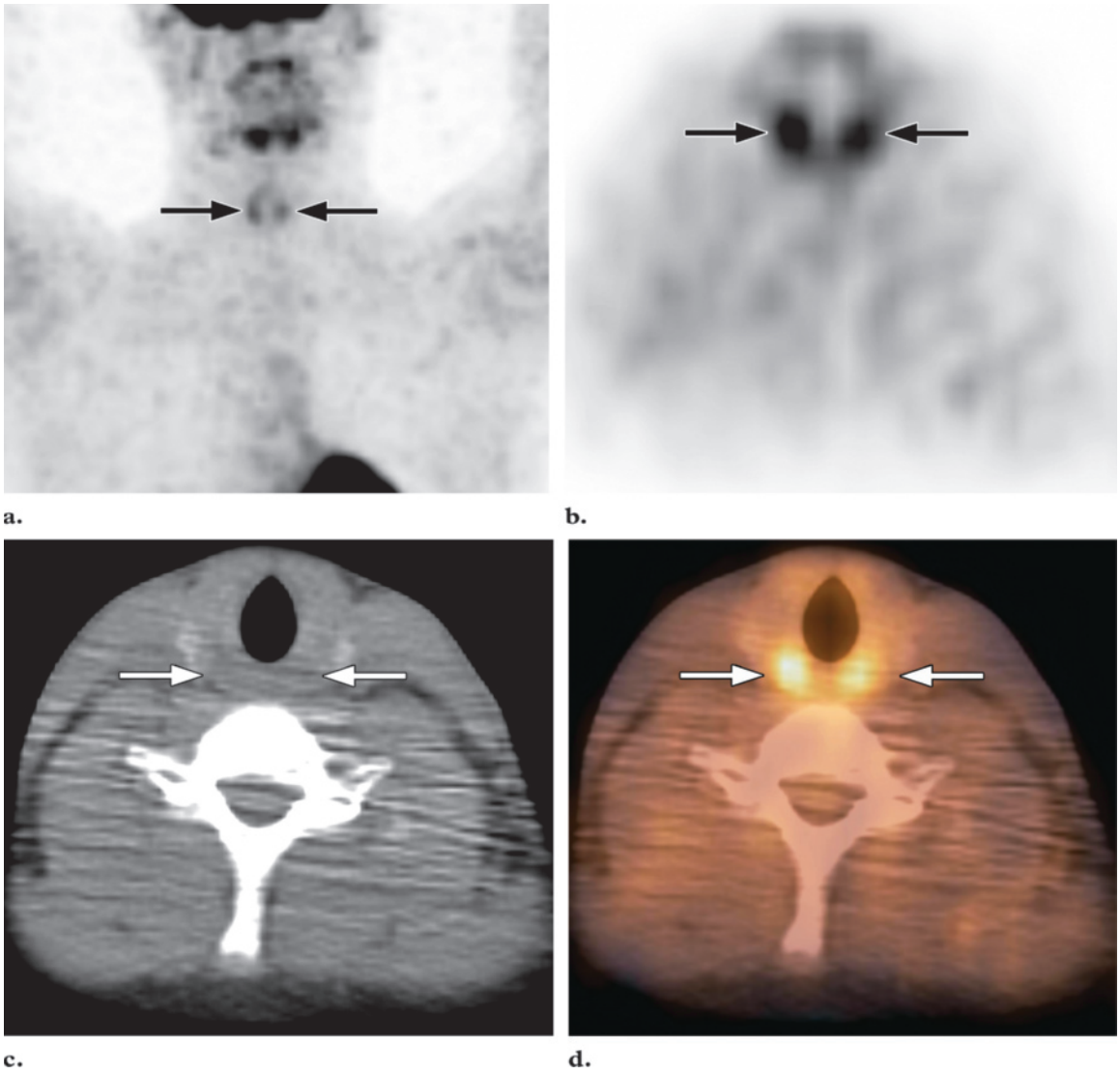

Figure 4. MIP FDG PET image **(a)** and transverse FDG PET **(b)**, CT **(c)**, and fused PET/CT **(d)** images show mildly increased uptake in the arytenoid muscles (arrows).

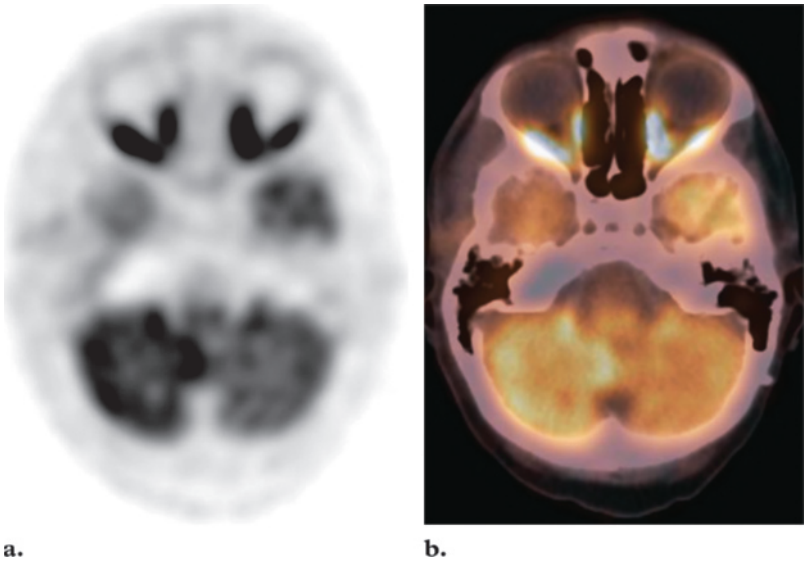

Figure 5. Transverse FDG PET scan **(a)** and fused PET/CT image **(b)** show bilateral marked uptake in the medial and lateral rectus muscles of the head.

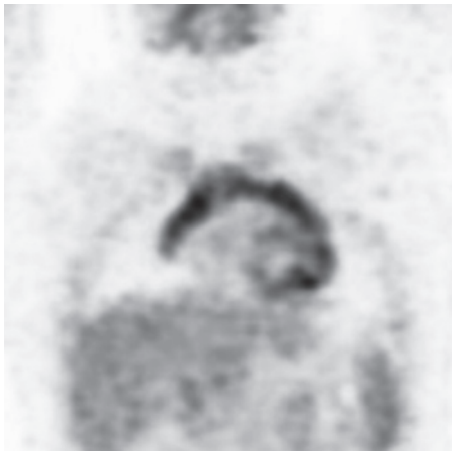

Figure 6. Coronal FDG PET scan shows diffuse and homogeneous uptake in the normal thymus. The uptake is bilobed with an inverted V shape.

Figure 7. MIP FDG PET image obtained in a patient who had eaten a heavy meal 3 hours prior to ^{18}F FDG injection shows intense uptake in the heart and high soft-tissue background activity.

Thymus

Teaching Point

Diffuse and homogeneous uptake in the thymus is common in healthy children (31). The uptake is bilobed with an inverted V shape on coronal views (Fig 6) (27). Generally, physiologic uptake in the thymus disappears during adolescence in conjunction with involution of the thymus (31). Prominent thymic uptake may also be seen following chemotherapy; homogeneous thymic uptake at posttherapy FDG PET and the absence of uptake at pretherapy FDG PET indicate posttherapy thymic hyperplasia. Thymic hyperplasia (or "rebound") is seen following chemotherapy more often in children than in adults. Brink et al (31) reported increased FDG accumulation in the thymus in 75% of children with malignant disease who had undergone chemotherapy. Very intense uptake or heterogeneous uptake may raise suspicion for thymic or other anterior mediastinal disease.

Myocardium

Cardiac activity is variable, ranging from no discernible activity above background blood pool activity, to intense activity throughout the left ventricular myocardium (10,30). The degree of cardiac uptake depends on substrate availability. During the fasting state, ^{18}F FDG uptake is low because *(a)* the predominant myocardial substrates are fatty acids as a source of energy, and *(b)* the serum insulin level is low. However, uptake can be variable or nonuniform even in the fasting state, a finding that may be misinterpreted as a mediastinal abnormality (10). In the postprandial state, when the serum glucose and insulin levels are high, myocardial uptake can be intense (Fig 7) (10,30). Therefore, in oncologic applications, cardiac activity is minimized by fasting for 4–6 hours prior to ^{18}F FDG injection. It is unusual to see atrial or right ventricular activity unless there is cardiac disease affecting those chambers (30,32). Increased ^{18}F FDG uptake has also been reported in lipomatous hypertrophy of the interatrial septum. The cause of this uptake may be related to the presence of brown fat (33).

Breast

Moderate and diffuse FDG uptake can be seen in normal breast due to proliferative glandular tissue (30). Higher uptake may be seen in adolescent girls with dense breasts. The nipples also normally demonstrate activity, which is better identified on non-attenuation-corrected images. Low-grade breast cancer might not be detected against this background activity (30). Lin et al (34) observed a significant correlation between the intensity of ^{18}F FDG uptake in normal breast tissue and the menstrual cycle. They postulated that ^{18}F FDG studies are less sensitive in detecting small breast tumors during the ovulatory and secretory phases. High ^{18}F FDG uptake can be seen in lactating breasts (35). The amount of radioactivity within breast milk is low, although most institutions recommend that breast feeding be discontinued for 8–24 hours after injection. The infant is more likely to receive radiation exposure from close contact with the breast than from milk (35).

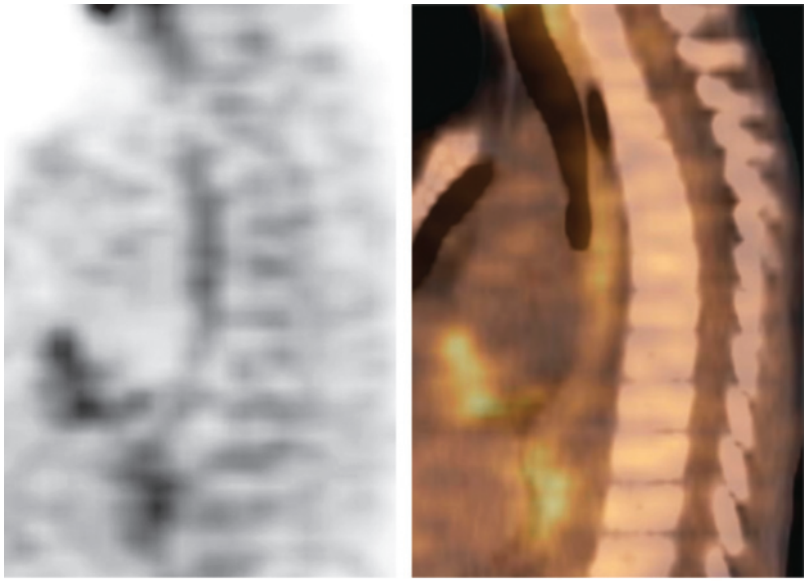

a. b.

Figure 8. Sagittal FDG PET scan **(a)** and fused PET/CT image **(b)** show linear ^{18}F FDG uptake anterior to the thoracic spine **(a)**, a finding that corresponds to the normal esophagus **(b)**.

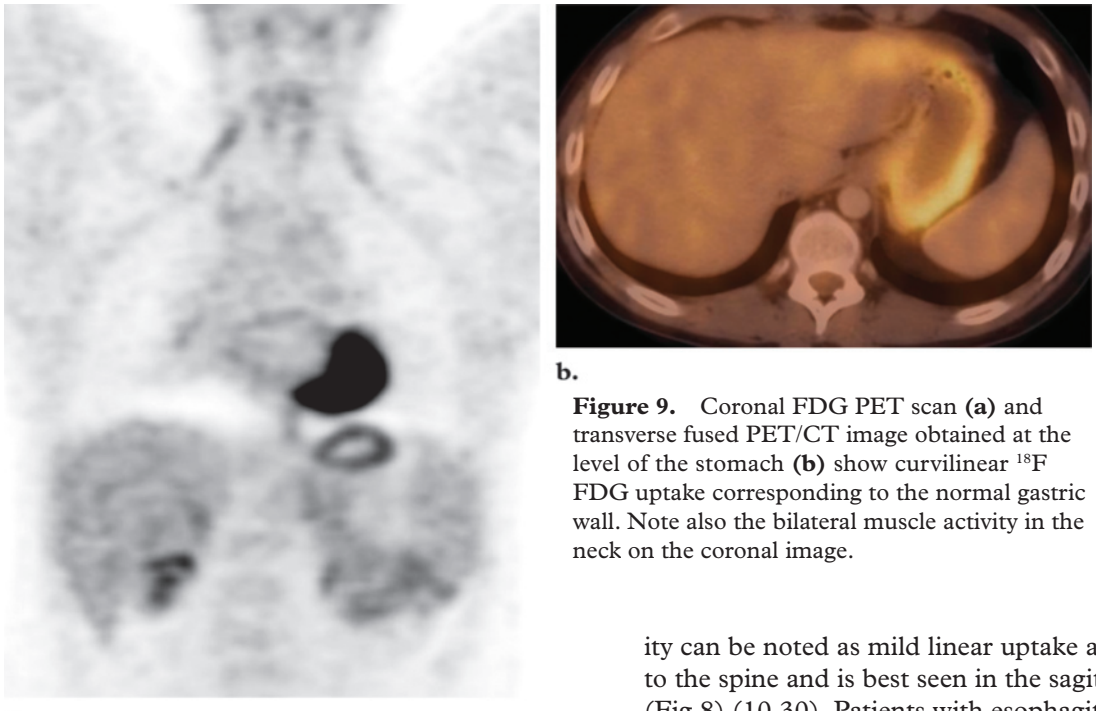

a. b.

Figure 9. Coronal FDG PET scan **(a)** and transverse fused PET/CT image obtained at the level of the stomach **(b)** show curvilinear ^{18}F FDG uptake corresponding to the normal gastric wall. Note also the bilateral muscle activity in the neck on the coronal image.

Gastrointestinal Tract

^{18}F FDG uptake in the normal gastrointestinal tract is highly variable and can range from mild to intense with a focal, diffuse, or segmental distribution. The origin of ^{18}F FDG uptake in the gastrointestinal tract is not fully understood and is likely multifactorial. It may be related to active smooth muscle, active mucosa, swallowed secretions, or microbial uptake (36). Esophageal activity can be noted as mild linear uptake anterior to the spine and is best seen in the sagittal plane (Fig 8) (10,30). Patients with esophagitis from reflux or after radiation therapy can have marked uptake along the esophagus. Patients with hiatal hernia and Barrett esophagus may also have increased uptake in the distal esophagus. Curvilinear homogeneous uptake corresponding to the gastric wall is commonly identified (Fig 9). If the stomach is contracted, a round area of moderate activity may be seen (28). Gastric uptake is usually mild, but more intense uptake may be associated with *Helicobacter pylori* infection (30).

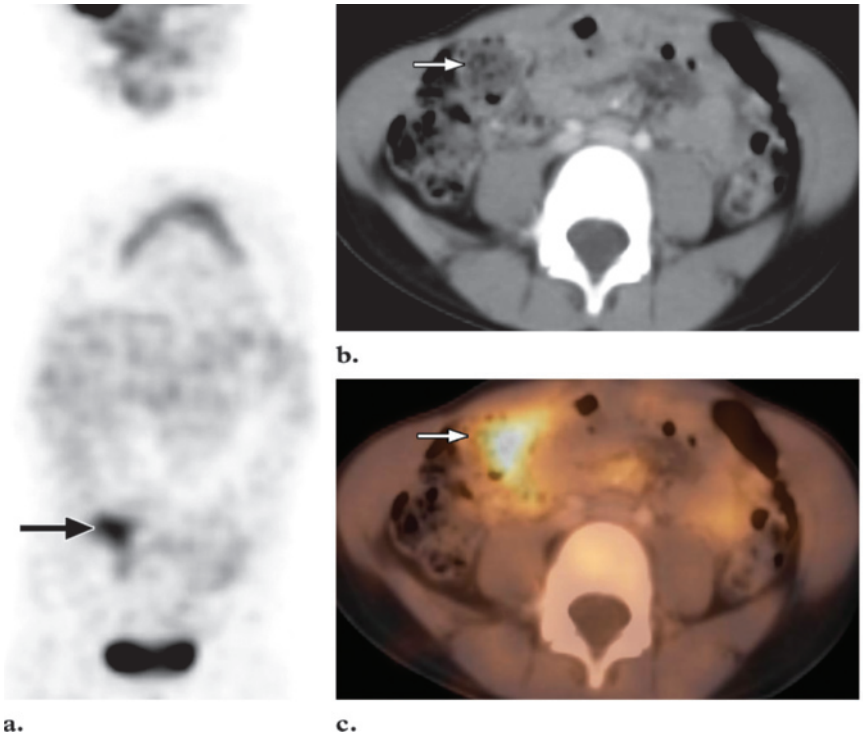

Figure 10. Coronal FDG PET scan **(a)** and transverse CT **(b)** and fused PET/CT **(c)** images show markedly increased ^{18}F FDG uptake in the normal right colon (arrow). Note also the physiologic uptake in the thymus on the coronal image.

Uptake in the small bowel is variable and is usually low grade when visible. Colonic activity is extremely variable and may be quite marked, affecting all or part of the colon. Uptake is typically more prominent in the cecum than in the rest of the colon, possibly due to a greater concentration of lymphoid tissue in the ileocecal region (Fig 10) (30,37). Occasionally, intense uptake in the cecum may make differentiation of malignancy or inflammation from a normal variant quite challenging. PET/CT can reduce diagnostic uncertainty by allowing direct anatomic correlation with normal bowel, leading to more confident image interpretation (37). Marked ^{18}F FDG accumulation can be seen in children with inflammatory bowel disease (38). The liver typically shows homogeneous moderate uptake, with relatively less intense uptake in the spleen.

Genitourinary System

Unlike glucose, ^{18}F FDG is not reabsorbed by the renal tubules, resulting in significant urinary activity in any part of the urinary tract. If there is significant retention in the renal collecting system, reconstruction artifacts may interfere with visualization of the upper abdomen (37). However, now that new iterative reconstruction algorithms are widely used, reconstruction artifacts from areas of high activity are less common than when filtered back projection was used (30). As discussed earlier, keeping the patient well hydrated and administering diuretics to dilute urinary activity can minimize such activity and improve image quality. The use of combined ^{18}F FDG PET/CT to localize foci of high ^{18}F FDG activity at CT helps avoid false-positive results due to urinary activity in the abdomen and pelvis (39). Significant activity along the entire length of the ureter is not typically seen in patients with a normal urinary tract but can be identified in those with obstruction or dilatation (37). Focal urinary activity within the ureter can resemble malignant lymphadenopathy (37,39). Urinary activity in bladder diverticula may mimic lymphadenopathy or ovarian tumors (37,39). Congenital variants such as ectopic kidney or horseshoe kidney and anatomic distortion such as urinary diversion may also lead to false-positive results (39).

In males, testicular uptake normally demonstrates a symmetric and diffuse pattern. The intensity is usually moderate and may decrease with age

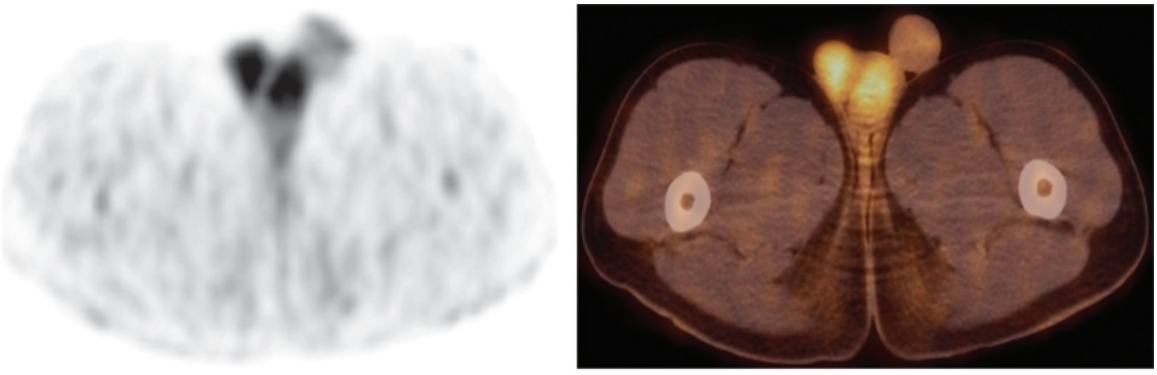

a. b.

Figure 11. Physiologic testicular uptake in a 16-year-old boy with a history of lymphoma of the left tibia. Transverse ^{18}F FDG PET scan **(a)** and fused PET/CT image **(b)** show moderate and diffuse uptake in the testicles. No abnormalities were seen at CT.

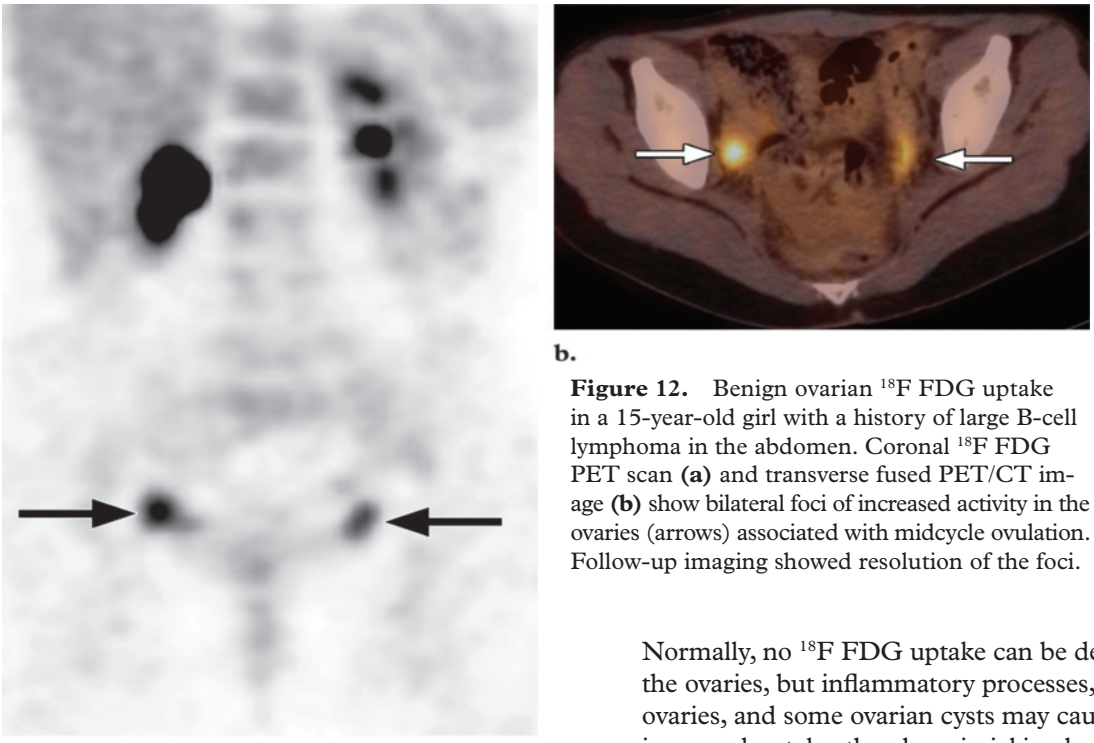

a. b.

Figure 12. Benign ovarian ^{18}F FDG uptake in a 15-year-old girl with a history of large B-cell lymphoma in the abdomen. Coronal ^{18}F FDG PET scan **(a)** and transverse fused PET/CT image **(b)** show bilateral foci of increased activity in the ovaries (arrows) associated with midcycle ovulation. Follow-up imaging showed resolution of the foci.

(Fig 11) (40). In females, the endometrium generally shows cyclically variable uptake, but marked uptake can be seen during menstruation (39). Lerman et al (41) observed two peaks of increased physiologic activity in premenopausal patients: one at midcycle and the other during the menstrual flow phase. Marked ^{18}F FDG uptake associated with fibroid tumors has also been reported (39).

Normally, no ^{18}F FDG uptake can be detected in the ovaries, but inflammatory processes, ovulating ovaries, and some ovarian cysts may cause focal increased uptake, thereby mimicking lymphadenopathy (Fig 12) (30,41). Focal increased uptake has also been described in physiologic corpus luteum cysts (Fig 13). The focal pattern of physiologic ovarian uptake can be misinterpreted as pelvic lymphadenopathy. Combined PET/CT allows precise anatomic localization of ^{18}F FDG uptake to ovarian structures, thereby improving differentiation of normal physiologic uptake from

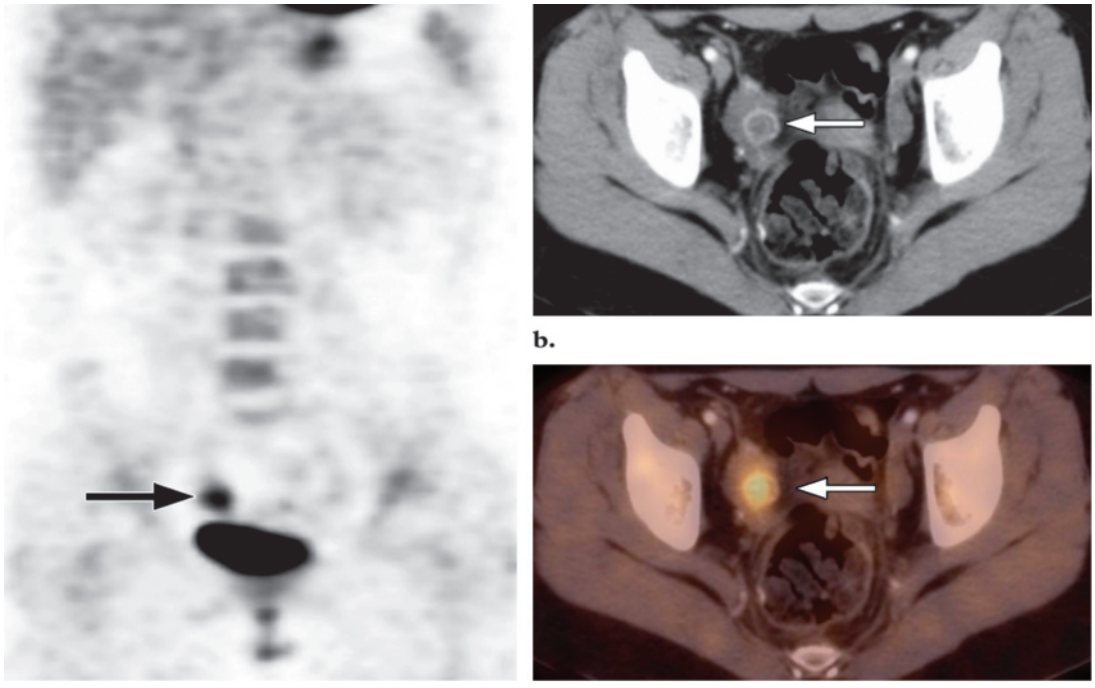

Figure 13. Ovarian corpus luteum cyst in a 17-year-old girl with a history of stage IVB Hodgkin disease. The patient's most recent menstrual period occurred 3 weeks prior to her undergoing follow-up ^{18}F FDG PET/CT after having completed chemotherapy. **(a)** Coronal FDG PET scan shows focal increased uptake in the right side of the pelvis (arrow). **(b)** Transverse CT scan shows a cystic structure with rim enhancement in the right ovary (arrow), a finding that is consistent with an ovarian corpus luteum cyst. **(c)** Transverse fused PET/CT image shows focal increased uptake in the cyst (arrow).

disease (42). Discussing the phase of the patient's menstrual cycle with her is often helpful in differentiating physiologic from malignant ovarian ^{18}F FDG uptake (41).

Skeletal Muscle

Generally, muscle uptake is low at rest. Physiologic muscle uptake is commonly encountered at ^{18}F FDG studies due to excessive muscle activity during the uptake phase or within a few days preceding the study (Fig 9) (43). High muscle uptake is most commonly seen in the head, neck, and thorax and less commonly in the lower extremities. The pattern is usually distinctive and symmetric in various muscle groups. However, asymmetric muscle uptake can occur. Marked uptake can be seen after excessive exercise or muscle tension. Laryngeal muscle uptake can be seen if the patient has been talking during the uptake phase (Fig 4). The chewing of gum after ^{18}F FDG injection can cause symmetric intense uptake in the masseter muscles. Uptake in these muscles may also be seen in babies who suck pacifiers during the uptake phase (16). Hyperventilation may induce diaphragmatic uptake. Uptake in the diaphragm, the crura of the diaphragm, and the intercostal muscles can be detected in children who have been crying during the uptake phase (Fig 14). Muscular imbalance after surgery or due to scoliosis may cause increased uptake in skeletal muscles due to altered mechanics. Insulin or recent food intake can cause diffuse skeletal muscle uptake, since insulin drives ^{18}F FDG into skeletal muscle. Muscle relaxants such as benzodiazepines may be used to minimize muscle uptake (44,45). To avoid marked muscle uptake, patients should rest comfortably during the uptake phase. Instructions may be given to children to avoid excessive exercise during the 48 hours prior to injection. Furthermore, technologists should discourage and report any excessive physical activity by the patient during the uptake phase (43).

Teaching Point

Brown Adipose Tissue

Physiologic high uptake can be observed along the distribution of activated brown adipose tissue in the neck, supraclavicular regions, axillae, mediastinum, and paravertebral and perinephric regions (Fig 15) (20). Uptake of ^{18}F FDG, a glucose

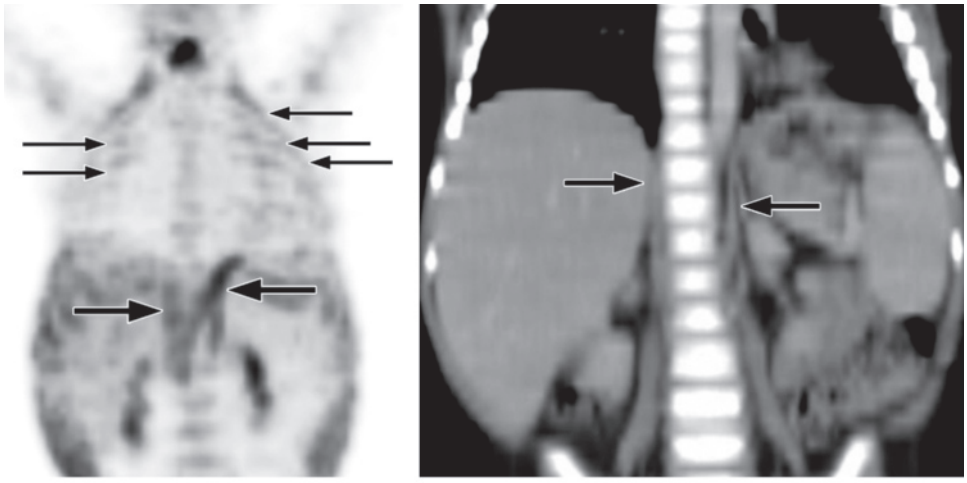

a. b.

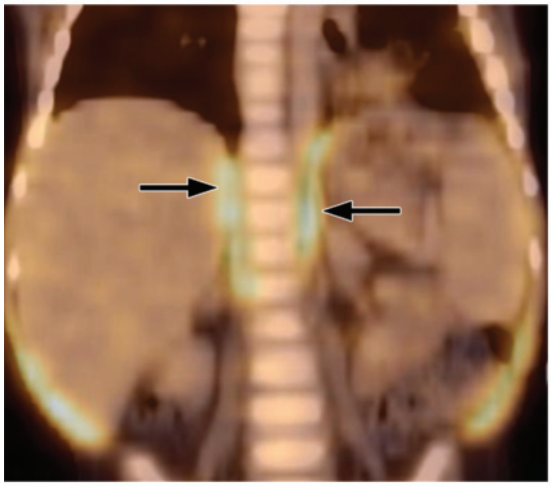

c.

Figure 14. Muscle uptake in a 2-year-old girl who was crying after ^{18}F FDG injection. **(a)** MIP FDG PET image shows increased uptake in the diaphragm and intercostal muscles (arrows). **(b)** Coronal CT scan shows no diaphragmatic abnormalities (arrows). **(c)** Coronal fused PET/CT image shows linear uptake (arrows) corresponding to the diaphragm (cf **b**).

Figure 15. MIP FDG PET image shows the typical distribution of uptake in brown adipose tissue in pediatric patients. The uptake is localized in the neck, supraclavicular and axillary regions, mediastinum, paravertebral and perinephric areas, and anterior abdominal wall.

analog, occurs when glucose transporters in brown adipose tissue have been activated (46). Since the introduction of PET, physiologic ^{18}F FDG uptake in activated brown adipose tissue has been known to be a source of false-positive results (45). ^{18}F FDG uptake in brown fat is typically bilateral and symmetric. However, focal and asymmetric uptake can occur in the neck or mediastinum, leading to false-positive results. Combined ^{18}F FDG PET/CT provides precise anatomic correlation, which allows differentiation between ^{18}F FDG uptake corresponding to fat-attenuation tissue at CT and uptake from pathologic causes (47). Uptake in brown fat is more common in children than in adults and is most common during the winter. Warming the patient prior to injection and during the uptake phase is a simple approach that is used routinely at our institution to reduce brown fat uptake (45,48). Brown fat ^{18}F FDG uptake can also be avoided by administering diazepam, fentanyl, or propanolol prior to injection (48,49).

Bone Marrow and Spleen

Generally, mild activity that is less intense than liver activity is identified within the hematopoietic bone marrow (30). Bone marrow activity that is more intense than liver activity is considered abnormal. Normal accumulation is generally homogeneous, with more extensive distribution in children than in adults (20). Increased bone marrow activity can be seen following chemotherapy, usually resolving within 1 month. Increased uptake can also be seen with hyperplasia and hematopoietic stimulation from anemia. Treatment with hematopoietic cytokines such as granulocyte colony-stimulating factor (CSF), hematopoietic growth factor, or erythropoietin can also produce diffuse skeletal ^{18}F FDG accumulation (Fig 16) (50). Increased activity can persist for up to 3 weeks after the discontinuation of granulocyte CSF treatment; therefore, it is advisable to postpone ^{18}F FDG PET until approximately 4 weeks after treatment (50).

Teaching Point

In addition, diffusely increased ^{18}F FDG uptake can be observed in the spleen during granulocyte CSF treatment, accompanying increased bone marrow uptake and reflecting granulocyte CSF–induced splenic extramedullary hematopoiesis (Fig 16) (51). It is important to recognize that increased splenic activity can also occur in patients with extrasplenic infection; therefore, splenic uptake should not automatically be interpreted as either splenic infection or tumor (13). The spleen is an integral part of the immune system and performs multiple tasks, including clearance of encapsulated bacteria, phagocytosis, and production of inflammatory substances and immunoglobulin antibodies. Presumably, diffusely increased splenic activity reflects increased glucose usage by this organ in the setting of extrasplenic infection (13).

Figure 16. Effect of granulocyte CSF treatment in a 15-year-old girl with Hodgkin disease. ^{18}F FDG PET/CT was performed after two cycles of chemotherapy. MIP FDG PET image shows diffuse skeletal and splenic uptake, a finding that reflects granulocyte CSF–induced hematopoiesis.

Reduced bone marrow ^{18}F FDG uptake can be noted several months after external beam radiation therapy. This phenomenon has been attributed to the replacement of bone marrow by fatty tissue (52). Typically, no ^{18}F FDG uptake is identified in normal bone. However, skeletally immature pediatric patients may have physiologic linear uptake in physes and apophyses (Fig 17) (53).

Teaching Point

Benign Causes of Abnormal ^{18}F FDG Uptake

^{18}F FDG is not a specific tumor agent and can accumulate in nonmalignant disorders, including infectious and inflammatory diseases (52).

Bone Lesions

Among benign bone lesions, fibro-osseous defects are of particular importance in children. Benign fibro-osseous lesions such as nonossifying fibro-

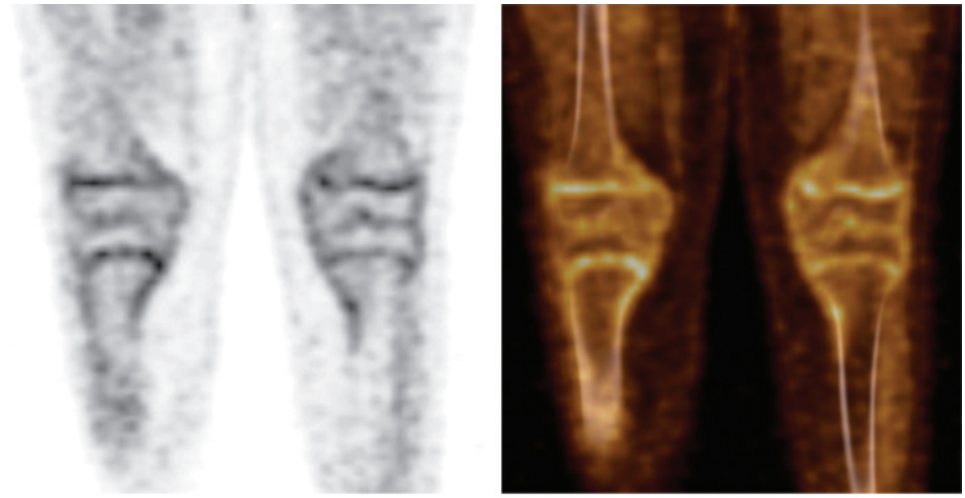

Figure 17. Coronal FDG PET scan **(a)** and fused PET/CT image **(b)** show bilateral linear ^{18}F FDG uptake in the distal femora and proximal tibiae, findings that correspond to the long bone physes.

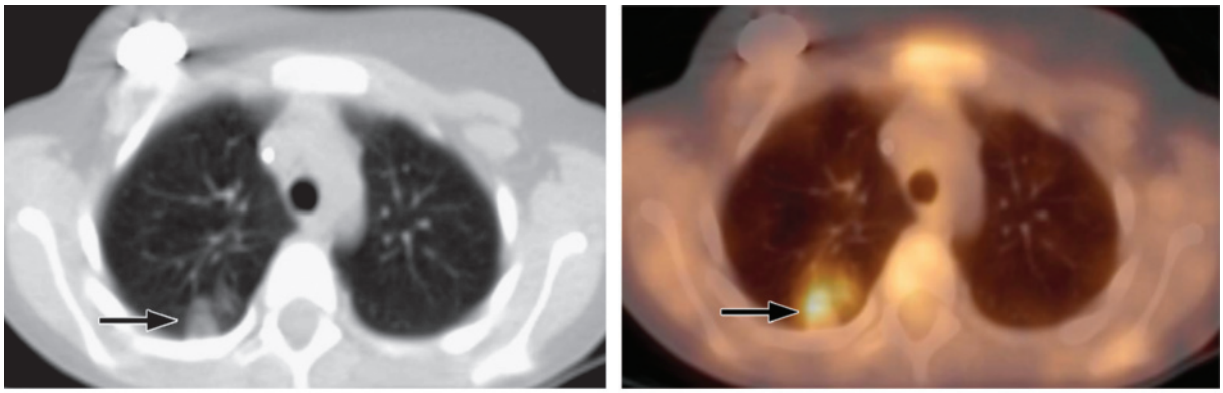

Figure 18. Pneumonia in an 8-year-old boy with a history of neuroblastoma, fever, and cough. **(a)** Transverse CT scan (lung window) shows an area of infection in the right lung (arrow). **(b)** Transverse fused ^{18}F FDG PET/CT image shows markedly increased uptake in the right lung (arrow), a finding that corresponds to the area of infection. At follow-up imaging performed after a course of antibiotic therapy, the infection had resolved.

mas, fibrous cortical defects, and cortical desmoid tumors can manifest with variably, often intensely, increased ^{18}F FDG uptake and thereby mimic malignant bone disease. Nonossifying fibromas and fibrous cortical defects are typically located in the metaphysis or diametaphyseal junction of the distal femur or proximal tibia. Correlation with the CT findings from a PET/CT study can help in characterizing these lesions and obviating further diagnostic procedures. CT will show an eccentric low-attenuation lesion with a thin sclerotic rim. It can also help determine whether a pathologic fracture has occurred (53). Acute or healing fractures may also show increased ^{18}F FDG activity. Osteoid osteoma, chondroblastoma, Langerhans cell histiocytosis, fibrous dysplasia, and osteomyelitis are other examples of pediatric bone lesions that can exhibit high FDG uptake (54,55).

Infection and Inflammation

Focal increased ^{18}F FDG accumulation is seen with various infectious or inflammatory processes, including abscesses, pneumonia, sinusitis, osteomyelitis, prosthetic joint infection, tuberculosis, infectious mononucleosis, and fungal or granulomatous disease such as aspergillosis, cryptococcosis, histoplasmosis, tuberculosis, Wegener granulomatosis, histiocytosis, and sarcoidosis. As noted earlier, ^{18}F FDG uptake has been reported in children with inflammatory bowel disease (12,13). Pneumonia may manifest with marked focal increased uptake in the lung, usually resolving after antibiotic therapy (Fig 18) (56). Foci of ^{18}F FDG accumulation in the gluteal muscles of the buttocks strongly suggest injection site

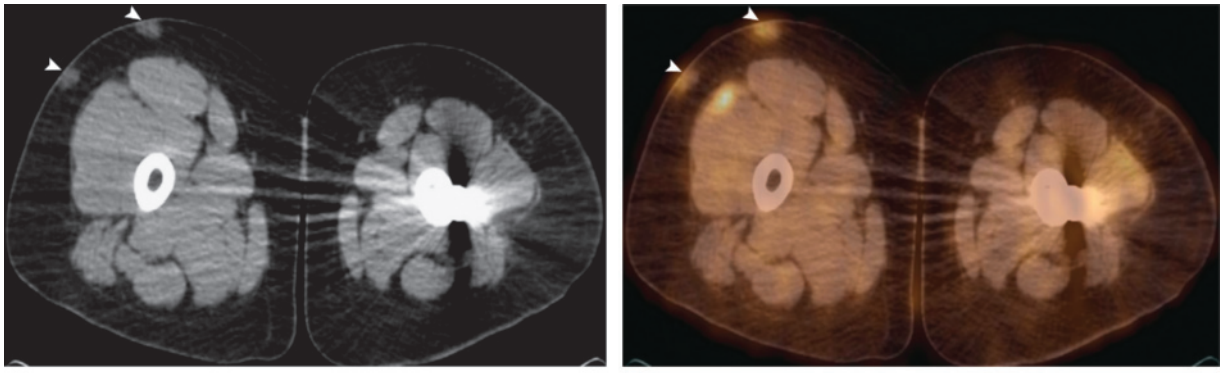

a. b.

Figure 19. FDG uptake at subcutaneous injection sites in a 16-year-old girl with a history of lymphoma and pathologic fracture of the proximal left femur. The patient had a history of prophylactic subcutaneous injections of low-molecular-weight heparin and had undergone hardware fixation. **(a)** Transverse CT scan obtained at the level of the thigh shows areas of soft-tissue attenuation (arrowheads). **(b)** Transverse fused PET/CT image shows foci of subcutaneous uptake (arrowheads) corresponding to the areas of soft-tissue attenuation seen at CT.

granulomas, especially in patients with a history of recent intramuscular injections. Injection site granulomas are also recognized after repeated injections of drugs into the subcutaneous fat (57). Patients receiving subcutaneous injections of low-molecular-weight heparin may develop FDG-avid subcutaneous areas of soft-tissue attenuation at the injection sites. Such nodules can resemble metastatic tumor deposits at CT (58). The accumulation of inflammatory cells and macrophages within these lesions may explain the ^{18}F FDG accumulation in the lesions. Careful correlation with clinical history is needed to avoid misdiagnosis (Fig 19) (57,58). Active vascular inflammation may demonstrate ^{18}F FDG uptake. ^{18}F FDG PET/CT images can help detect Takayasu arteritis and reflect the distribution of inflammatory activity in the vascular wall (59).

Technical Artifacts

The use of a combined PET/CT imaging system creates distinctive artifacts that are not seen on dedicated PET-only systems. The most commonly seen artifacts are related to the use of CT data rather than PET data for attenuation correction. Metallic objects such as prostheses, pacemakers, or chemotherapy catheters can cause artifactually increased activity and lead to false-positive results (Fig 20) (20,60). The high CT attenuation values (in Hounsfield units) cause falsely high PET attenuation coefficients, leading to overestimation of the PET activity corresponding to the metallic objects on the attenuation-corrected images (30,60). Similarly, highly concentrated intravenous and oral contrast material can lead to overcorrection of activity and false-positive results at PET if enhanced

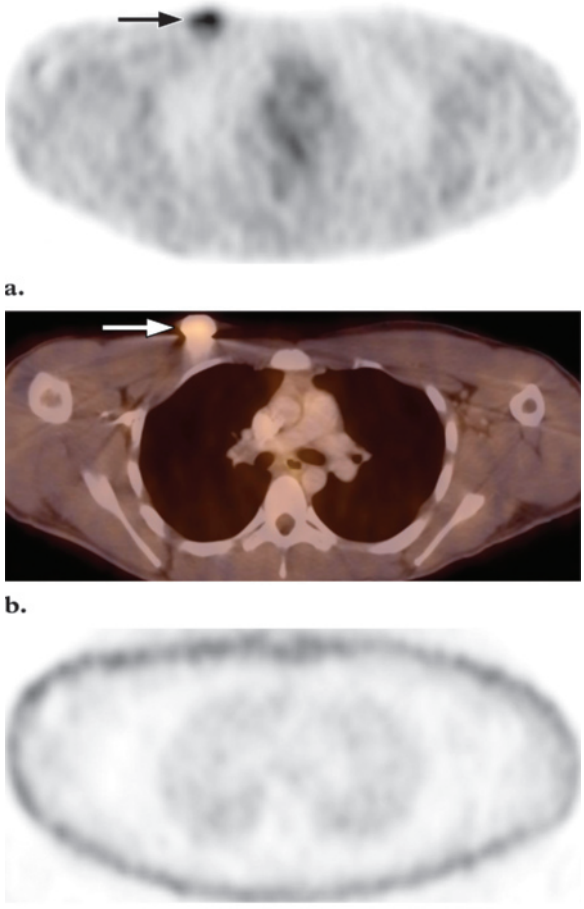

a.

b.

c.

Figure 20. Attenuation correction artifact. **(a)** Transverse attenuation-corrected FDG PET scan shows a focus of increased uptake in the upper right chest wall (arrow). **(b)** Transverse fused PET/CT image also shows the focus of increased uptake (arrow), a finding that represents a catheter. **(c)** Transverse non-attenuation-corrected FDG PET scan shows no increased uptake. The high attenuation of a catheter leads to overcorrection of the activity on attenuation-corrected images. This artifact is not present on non-attenuation-corrected images.

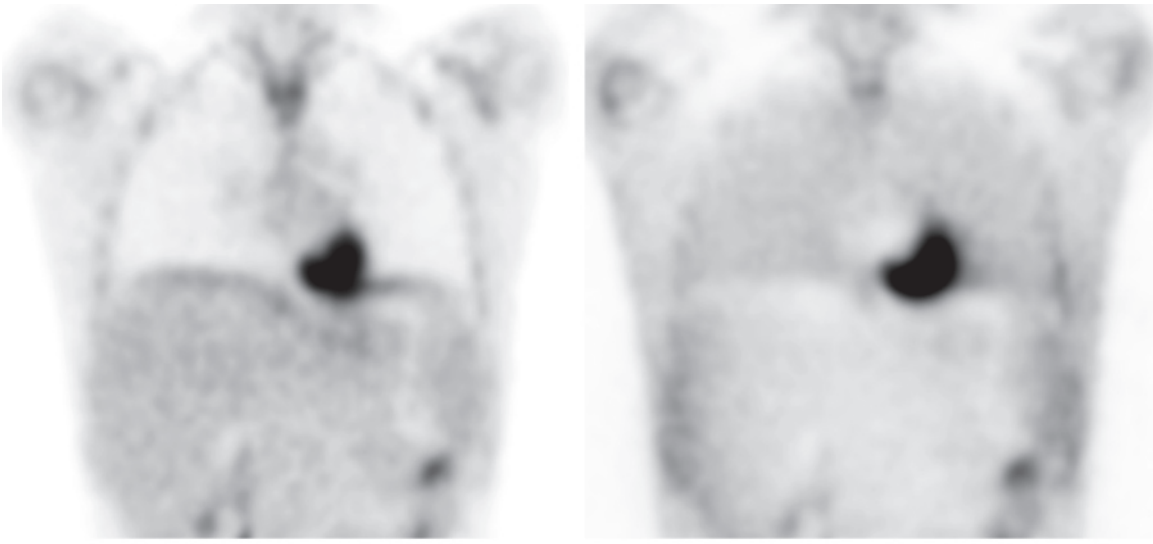

a. b.

Figure 21. Respiratory motion artifact. **(a)** Coronal attenuation-corrected FDG PET scan shows bilateral curvilinear uptake along the domes of the diaphragm. **(b)** Coronal non-attenuation-corrected FDG PET scan shows no abnormally increased activity, a finding that, along with the fact that there was no corresponding CT abnormality, confirms that the diaphragmatic uptake seen in **a** represents respiratory motion artifact.

CT data are used for attenuation correction. Overly concentrated intravenous contrast material is typically seen in the region just proximal to the intravenous catheter (eg, upper arm and axilla after antecubital injection). Overly concentrated oral contrast material usually represents retained barium in the colon after a recent fluoroscopic or CT examination. Viewing the non-attenuation-corrected PET images can help distinguish this attenuation correction artifact from true hypermetabolism, since this artifactually high activity will not be present on the noncorrected images (30,60). Oral contrast material may not significantly affect image quality and visual interpretation. However, semiquantitative measures such as standardized uptake value (SUV) may be affected slightly (20). Intravenous contrast material can also result in the overestimation of PET attenuation factors and an increase in SUV in regions of highly concentrated contrast material. However, this increase may be clinically insignificant, and PET/CT with intravenous contrast-enhanced CT can be used in combination with PET to evaluate patients with cancer (23,24). The optimal method for calculating SUV in children may be different from that used in adults due to the body changes and growth that take place during childhood. Therefore, it has been suggested that, in pediatric patients, SUV calculated on the basis of body surface area would serve as a better metabolic activity marker than would SUV calculated on the basis of body weight and is probably the most appropriate approach for the follow-up of these patients, assuming that SUVs are to be used (61).

Respiratory motion in children can cause misregistration of PET and CT scans, leading to attenuation correction artifact. The liver dome and spleen may be seen above the diaphragm at CT, there may be crescentic areas of photopenia above the diaphragm ("banana sign"), or focal uptake in the dome of the liver may be falsely localized to the lung base on the attenuation-corrected images, thereby mimicking a lung nodule (Fig 21). These artifacts are due to the difference in diaphragm position at CT and PET. PET is performed over several minutes during tidal breathing, with the final PET scan depicting the average position of the diaphragm during respiration. In contrast, CT is performed during a specific stage of the breathing cycle—usually full inspiration, when the diaphragm is at its lowest point (60). Misregistration may be minimized by performing CT during midexpiration (30). Any change in patient position between PET and CT can lead to misregistration on the fusion images and attenuation artifact on the attenuation-corrected images (Fig 22).

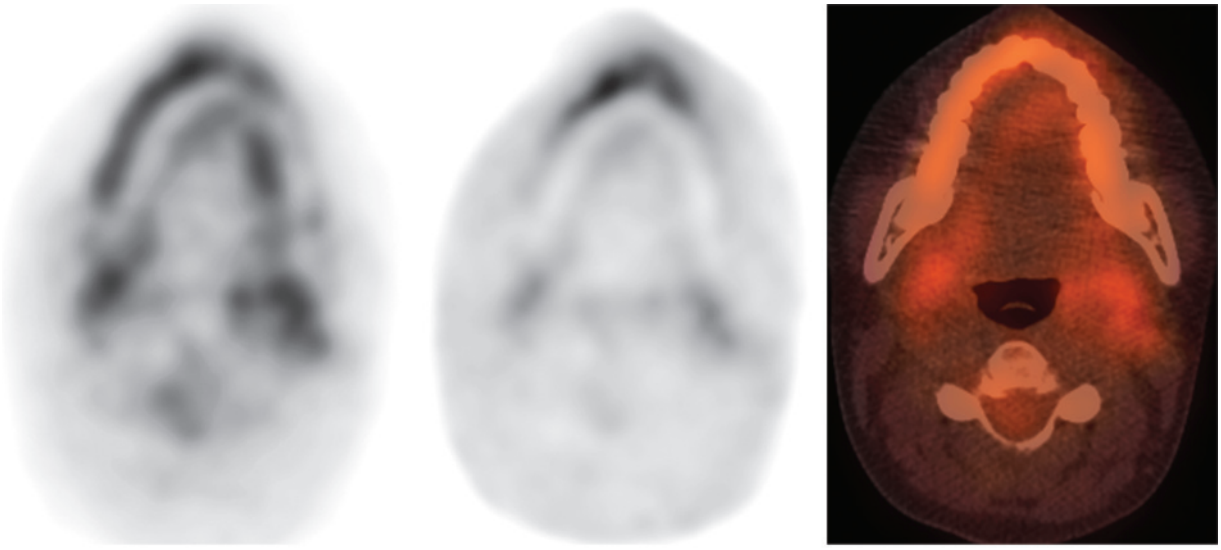

a. b. c.

Figure 22. Motion artifact in a 16-year-old girl. **(a)** Transverse attenuation-corrected FDG PET scan shows artifactually high uptake along the outer aspect of the right mandibular body and along the inner aspect of the left mandibular body. **(b)** Non-attenuation-corrected FDG PET scan shows symmetric mandibular uptake. **(c)** Fused FDG PET/CT image shows artifactually high uptake corresponding to that shown in **a**. The symmetric mandibular uptake shown on the non-attenuation-corrected scan, along with the fact that there was no corresponding abnormality at CT, confirms that the uptake seen in **a** and **c** represents motion artifact.

The CT scanner may have a relatively smaller-diameter field of view (50 cm) compared with the PET scanner (70 cm). This difference can lead to truncation artifacts when the patient's body extends beyond the CT field of view, causing underestimation of the SUV of the peripheral portions of the attenuated-corrected images. In addition, truncation can cause streak artifact at the edges of the CT scans and overestimation on the attenuation-corrected images, producing high activity at the edges. Therefore, it is important for technologists to ensure that the patient is at the center of the field of view and that the patient's entire body is included, especially in morbidly obese children (positioning the child's arms above the head may be helpful), to reduce truncation artifacts (60). If it is technically impossible to include the entire body in the field of view, the patient should be positioned in such a way that any body parts of specific clinical concern are completely included.

Summary

Combined ^{18}F FDG PET/CT is being used more frequently in the evaluation of pediatric patients with cancer. Many of the normal variants in children are similar to those in adults. However, the normal distribution of ^{18}F FDG uptake in children is unique and may differ from that in adults, such as the physiologic activity of the lymphatic tissue in the Waldeyer ring, as well as uptake in the ileocecal region, thymus, hematopoietic bone marrow, and skeletal growth centers. To appropriately interpret an ^{18}F FDG PET/CT study, it is essential to be familiar with the normal physiologic distribution of ^{18}F FDG uptake in children and to recognize physiologic variants, artifacts, and potential pitfalls. Knowing these potential causes of misinterpretation can increase accuracy in PET image interpretation, decrease the number of unnecessary follow-up studies or procedures, and improve patient treatment. Misinterpretation can also be minimized with proper patient preparation, a complete clinical history of the patient, and correlation with anatomic imaging. The use of combined ^{18}F FDG PET/CT brings to light many pitfalls and normal variants by allowing the precise localization of functional ^{18}F FDG PET data on conventional anatomic CT data.

References

1. Hustinx R, Bénard F, Alavi A. Whole-body FDG-PET imaging in the management of patients with cancer. Semin Nucl Med 2002;32(1):35–46.
2. Gambhir SS, Czernin J, Schwimmer J, Silverman DH, Coleman RE, Phelps ME. A tabulated summary of the FDG PET literature. J Nucl Med 2001; 42(suppl):1S–93S.

3. Hillner BE, Siegel BA, Liu D, et al. Impact of positron emission tomography/computed tomography and positron emission tomography (PET) alone on expected management of patients with cancer: initial results from the National Oncologic PET Registry. J Clin Oncol 2008;26(13):2155–2161. [Published correction appears in J Clin Oncol 2008;26(25):4229.]
4. Tatsumi M, Miller JH, Wahl RL. 18F-FDG PET/CT in evaluating non-CNS pediatric malignancies. J Nucl Med 2007;48(12):1923–1931.
5. Depas G, De Barsy C, Jerusalem G, et al. 18F-FDG PET in children with lymphomas. Eur J Nucl Med Mol Imaging 2005;32(1):31–38.
6. Shulkin BL, Mitchell DS, Ungar DR, et al. Neoplasms in a pediatric population: 2-[F-18]-fluoro-2-deoxy-D-glucose PET studies. Radiology 1995;194(2):495–500.
7. Franzius C, Schober O. Assessment of therapy response by FDG PET in pediatric patients. Q J Nucl Med 2003;47(1):41–45.
8. Hudson MM, Krasin MJ, Kaste SC. PET imaging in pediatric Hodgkin's lymphoma. Pediatr Radiol 2004;34(3):190–198.
9. O'Hara SM, Donnelly LF, Coleman RE. Pediatric body applications of FDG PET. AJR Am J Roentgenol 1999;172(4):1019–1024.
10. Abouzied MM, Crawford ES, Nabi HA. 18F-FDG imaging: pitfalls and artifacts. J Nucl Med Technol 2005;33(3):145–155.
11. Pauwels EK, Ribeiro MJ, Stoot JH, McCready VR, Bourguignon M, Mazière B. FDG accumulation and tumor biology. Nucl Med Biol 1998;25(4):317–322.
12. Zhuang H, Alavi A. 18-fluorodeoxyglucose positron emission tomographic imaging in the detection and monitoring of infection and inflammation. Semin Nucl Med 2002;32(1):47–59.
13. Love C, Tomas MB, Tronco GG, Palestro CJ. FDG PET of infection and inflammation. RadioGraphics 2005;25(5):1357–1368.
14. Kubota R, Yamada S, Kubota K, Ishiwata K, Tamahashi N, Ido T. Intratumoral distribution of fluorine-18-fluorodeoxyglucose in vivo: high accumulation in macrophages and granulation tissues studied by microautoradiography. J Nucl Med 1992;33(11):1972–1980.
15. Rennen HJ, Boerman OC, Oyen WJ, Corstens FH. Scintigraphic imaging of inflammatory processes. Curr Med Chem 2002;1(1):63–75.
16. Stauss J, Franzius C, Pfluger T, et al. Guidelines for 18F-FDG PET and PET-CT imaging in paediatric oncology. Eur J Nucl Med Mol Imaging 2008;35(8):1581–1588.
17. Shulkin BL, Hutchinson RJ, Castle VP, Yanik GA, Shapiro B, Sisson JC. Neuroblastoma: positron emission tomography with 2-[fluorine-18]fluoro-2-deoxy-D-glucose compared with metaiodobenzylguanidine scintigraphy. Radiology 1996;199(3):743–750.
18. Barrington SF, Begent J, Lynch T, et al. Guidelines for the use of PET-CT in children. Nucl Med Commun 2008;29(5):418–424.
19. Delbeke D, Coleman RE, Guiberteau MJ, et al. Procedure guideline for tumor imaging with 18F-FDG PET/CT 1.0. J Nucl Med 2006;47(5):885–895.
20. Jadvar H, Connolly LP, Fahey FH, Shulkin BL. PET and PET/CT in pediatric oncology. Semin Nucl Med 2007;37(5):316–331.
21. Brix G, Lechel U, Glatting G, et al. Radiation exposure of patients undergoing whole-body dual-modality 18F-FDG PET/CT examinations. J Nucl Med 2005;46(4):608–613.
22. Fahey FH, Palmer MR, Strauss KJ, Zimmerman RE, Badawi RD, Treves ST. Dosimetry and adequacy of CT-based attenuation correction for pediatric PET: phantom study. Radiology 2007;243(1):96–104.
23. Mawlawi O, Erasmus JJ, Munden RF, et al. Quantifying the effect of IV contrast media on integrated PET/CT: clinical evaluation. AJR Am J Roentgenol 2006;186(2):308–319.
24. Yau YY, Chan WS, Tam YM, et al. Application of intravenous contrast in PET-CT: does it really introduce significant attenuation correction error? J Nucl Med 2005;46(2):283–291.
25. Berthelsen AK, Holm S, Loft A, Klausen TL, Andersen F, Højgaard L. PET/CT with intravenous contrast can be used for PET attenuation correction in cancer patients. Eur J Nucl Med Mol Imaging 2005;32(10):1167–1175.
26. Ak I, Stokkel MP, Pauwels EK. Positron emission tomography with 2-[18F]fluoro-2-deoxy-D-glucose in oncology. II. The clinical value in detecting and staging primary tumours. J Cancer Res Clin Oncol 2000;126(10):560–574.
27. Burrell SC, Van den Abbeele AD. 2-Deoxy-2-[F-18]fluoro-D-glucose-positron emission tomography of the head and neck: an atlas of normal uptake and variants. Mol Imaging Biol 2005;7(3):244–256.
28. Sarji SA. Physiological uptake in FDG PET simulating disease. Biomed Imaging Interv J 2006;2(4):e59.
29. Nakamoto Y, Tatsumi M, Hammoud D, Cohade C, Osman MM, Wahl RL. Normal FDG distribution patterns in the head and neck: PET/CT evaluation. Radiology 2005;234(3):879–885.
30. Cook GJ, Wegner EA, Fogelman I. Pitfalls and artifacts in 18FDG PET and PET/CT oncologic imaging. Semin Nucl Med 2004;34(2):122–133.
31. Brink I, Reinhardt MJ, Hoegerle S, Altehoefer C, Moser E, Nitzsche EU. Increased metabolic activity in the thymus studied with FDG PET: age dependency and frequency after chemotherapy. J Nucl Med 2001;42(4):591–595.
32. Fujii H, Ide M, Yasuda S, Takahashi W, Shohtsu A, Kubo A. Increased FDG uptake in the wall of the right atrium in people who participated in a cancer screening program with whole-body PET. Ann Nucl Med 1999;13(1):55–59.
33. Fan CM, Fischman AJ, Kwek BH, Abbara S, Aquino SL. Lipomatous hypertrophy of the interatrial septum: increased uptake on FDG PET. AJR Am J Roentgenol 2005;184(1):339–342.
34. Lin CY, Ding HJ, Liu CS, Chen YK, Lin CC, Kao CH. Correlation between the intensity of breast FDG uptake and menstrual cycle. Acad Radiol 2007;14(8):940–944.
35. Hicks RJ, Binns D, Stabin MG. Pattern of uptake and excretion of 18F-FDG in the lactating breast. J Nucl Med 2001;42(8):1238–1242.
36. Shreve PD, Anzai Y, Wahl RL. Pitfalls in oncologic diagnosis with FDG PET imaging: physiologic and benign variants. RadioGraphics 1999;19(1):61–77.

37. Cook GJ, Fogelman I, Maisey MN. Normal physiological and benign pathological variants of 18-fluoro-2-deoxyglucose positron-emission tomography scanning: potential for error in interpretation. Semin Nucl Med 1996;26(4):308–314.
38. Löffler M, Weckesser M, Franzius C, Schober O, Zimmer KP. High diagnostic value of 18F-FDG-PET in pediatric patients with chronic inflammatory bowel disease. Ann N Y Acad Sci 2006;1072:379–385.
39. Subhas N, Patel PV, Pannu HK, Jacene HA, Fishman EK, Wahl RL. Imaging of pelvic malignancies with in-line FDG PET-CT: case examples and common pitfalls of FDG PET. RadioGraphics 2005;25(4):1031–1043.
40. Kitajima K, Nakamoto Y, Senda M, Onishi Y, Okizuka H, Sugimura K. Normal uptake of 18F-FDG in the testis: an assessment by PET/CT. Ann Nucl Med 2007;21(7):405–410.
41. Lerman H, Metser U, Grisaru D, Fishman A, Lievshitz G, Even-Sapir E. Normal and abnormal 18F-FDG endometrial and ovarian uptake in pre- and postmenopausal patients: assessment by PET/CT. J Nucl Med 2004;45(2):266–271.
42. Ames J, Blodgett T, Meltzer C. 18F-FDG uptake in an ovary containing a hemorrhagic corpus luteal cyst: false-positive PET/CT in a patient with cervical carcinoma. AJR Am J Roentgenol 2005;185(4):1057–1059.
43. Jackson RS, Schlarman TC, Hubble WL, Osman MM. Prevalence and patterns of physiologic muscle uptake detected with whole-body 18F-FDG PET. J Nucl Med Technol 2006;34(1):29–33.
44. Barrington SF, Maisey MN. Skeletal muscle uptake of fluorine-18-FDG: effect of oral diazepam. J Nucl Med 1996;37(7):1127–1129.
45. Yeung HW, Grewal RK, Gonen M, Schoder H, Larsen SM. Patterns of (18)F-FDG uptake in adipose tissue and muscle: a potential source of false-positives for PET. J Nucl Med 2003;44(11):1789–1796.
46. Kawashita NH, Brito MN, Brito SR, et al. Glucose uptake, glucose transporter GLUT4, and glycolytic enzymes in brown adipose tissue from rats adapted to a high-protein diet. Metabolism 2002;51(11):1501–1505.
47. Truong MT, Erasmus JJ, Munden RF, et al. Focal FDG uptake in mediastinal brown fat mimicking malignancy: a potential pitfall resolved on PET/CT. AJR Am J Roentgenol 2004;183(4):1127–1132.
48. Gelfand MJ, O'Hara SM, Curtwright LA, Maclean JR. Pre-medication to block [(18)F]FDG uptake in the brown adipose tissue of pediatric and adolescent patients. Pediatr Radiol 2005;35(10):984–990.
49. Parysow O, Mollerach AM, Jager V, Racioppi S, San Roman J, Gerbaudo VH. Low-dose oral propranolol could reduce brown adipose tissue F-18 FDG uptake in patients undergoing PET scans. Clin Nucl Med 2007;32(5):351–357.
50. Kazama T, Swanston N, Podoloff DA, Macapinlac HA. Effect of colony-stimulating factor and conventional- or high-dose chemotherapy on FDG uptake in bone marrow. Eur J Nucl Med Mol Imaging 2005;32(12):1406–1411.
51. Sugawara Y, Zasadny KR, Kison PV, Baker LH, Wahl RL. Splenic fluorodeoxyglucose uptake increased by granulocyte colony-stimulating factor therapy: PET imaging results. J Nucl Med 1999;40(9):1456–1462.
52. Alavi A, Gupta N, Alberini JL, et al. Positron emission tomography imaging in nonmalignant thoracic disorders. Semin Nucl Med 2002;32(4):293–321.
53. Goodin GS, Shulkin BL, Kaufman RA, McCarville MB. PET/CT characterization of fibroosseous defects in children: 18F-FDG uptake can mimic metastatic disease. AJR Am J Roentgenol 2006;187(4):1124–1128.
54. Aoki J, Watanabe H, Shinozaki T, et al. FDG PET of primary benign and malignant bone tumors: standardized uptake value in 52 lesions. Radiology 2001;219(3):774–777.
55. Schulte M, Brecht-Krauss D, Heymer B, et al. Grading of tumors and tumorlike lesions of bone: evaluation by FDG PET. J Nucl Med 2000;41(10):1695–1701.
56. Kapucu LO, Meltzer CC, Townsend DW, Keenan RJ, Luketich JD. Fluorine-18-fluorodeoxyglucose uptake in pneumonia. J Nucl Med 1998;39(7):1267–1269.
57. Prosch H, Mirzaei S, Oschatz E, Strasser G, Huber M, Mostbeck G. Gluteal injection site granulomas: false positive finding on FDG-PET in patients with non-small cell lung cancer. Br J Radiol 2005;78(932):758–761.
58. Funt SA, Hidalgo A, Panicek DM. Subcutaneous nodules at the injection site of low-molecular-weight heparin: a mimic of metastatic disease at CT. J Comput Assist Tomogr 2002;26(4):520–523.
59. Kobayashi Y, Ishii K, Oda K, et al. Aortic wall inflammation due to Takayasu arteritis imaged with 18F-FDG PET coregistered with enhanced CT. J Nucl Med 2005;46(6):917–922.
60. Sureshbabu W, Mawlawi O. PET/CT imaging artifacts. J Nucl Med Technol 2005;33(3):156–164.
61. Yeung HW, Sanches A, Squire OD, Macapinlac HA, Larson SM, Erdi YE. Standardized uptake value in pediatric patients: an investigation to determine the optimum measurement parameter. Eur J Nucl Med Mol Imaging 2002;29(1):61–66.

Pediatric FDG PET/CT: Physiologic Uptake, Normal Variants, and Benign Conditions

Amer Shammas, MD, et al

RadioGraphics 2009; 29:1467–1486 • **Published online** 10.1148/rg.295085247 • **Content Codes:** CT NM PD

Page 1471
[M]arkedly intense uptake can be seen in the Waldeyer ring (Fig 2) (27)—especially in children, due to high physiologic activity of these lymphatic tissues that peaks at 6–8 years of age, after which time it diminishes. These areas of normal F-18 FDG activity in children should not necessarily be interpreted as disease.

Page 1474
Diffuse and homogeneous uptake in the thymus is common in healthy children (31). The uptake is bilobed with an inverted V shape on coronal views (Fig 6) (27).

Page 1478
Hyperventilation may induce diaphragmatic uptake. Uptake in the diaphragm, the crura of the diaphragm, and the intercostal muscles can be detected in children who have been crying during the uptake phase (Fig 14).

Page 1480
Bone marrow activity that is more intense than liver activity is considered abnormal. Normal accumulation is generally homogeneous, with more extensive distribution in children than in adults (20).

Page 1480
Typically, no F-18 FDG uptake is identified in normal bone. However, skeletally immature pediatric patients may have physiologic linear uptake in physes and apophyses (Fig 17) (53).